Published OnlineFirst August 13, 2019; DOI: 10.1158/0008-5472.CAN-18-3880

Molecular Cell Biology

Cancer Research

Long Noncoding RNA MIR17HG Promotes Colorectal Cancer Progression via miR-17-5p

Jie Xu[1], Qingtao Meng[1], Xiaobo Li[1], Hongbao Yang[2], Jin Xu[3], Na Gao[1], Hao Sun[1], Shenshen Wu[1], Giuseppe Familiari[4], Michela Relucenti[4], Haitao Zhu[5], Jiong Wu[6], and Rui Chen[1,7]

Abstract

Immune dysregulation plays a vital role in colorectal cancer initiation and progression. Long noncoding RNAs (lncRNA) exhibit multiple functions including regulation of gene expression. Here, we identified an immune-related lncRNA, MIR17HG, whose expression was gradually upregulated in adjacent, adenoma, and colorectal cancer tissue. MIR17HG promoted tumorigenesis and metastasis in colorectal cancer cells both *in vitro* and *in vivo*. Mechanistically, MIR17HG increased the expression of NF-κB/RELA by competitively sponging the microRNA miR-375. In addition, RELA transcriptionally activated MIR17HG in a positive feedback loop by directly binding to its promoter region. Moreover, miR-17-5p, one of the transcribed miRNAs from MIR17HG, reduced the expression of the tumor suppressor B-cell linker (BLNK), resulting in increased migration and invasion of colorectal cancer cells. MIR17HG also upregulated PD-L1, indicating its potential role in immunotherapy. Overall, these findings demonstrate that MIR17HG plays an oncogenic role in colorectal cancer and may serve as a promising therapeutic target.

Significance: These findings provide mechanistic insight into the role of the lncRNA MIR17HG and its miRNA members in regulating colorectal cancer carcinogenesis and progression.

Introduction

Colorectal cancer is a severe health threat worldwide (1). Although remarkable progress has been made in the past decades, the molecular mechanisms underlying colorectal cancer carcinogenesis and progression remain unclear. Thus, novel biomarkers for early screening and therapeutic intervention are urgently demanded. In previous studies, the association between chronic inflammation and colorectal cancer has been extensively exploited (2). NF-κB is a master regulator of inflammation and inflammation-associated cancer (3). NF-κB promotes the secretion of proinflammatory cytokines and regulates the cell cycle and survival of colorectal cancer cells (4, 5). Given its importance, NF-κB and its upstream and downstream networks present potential targets for therapeutic interventions.

Long noncoding RNAs (lncRNA) are a class of transcripts longer than 200 nucleotides with little protein-coding capacity (6). Massive evidence suggests that lncRNAs are implicated in various biological processes of cancer, including differentiation, proliferation, apoptosis, metastasis, and drug resistance (6–8). Although several lncRNAs and their underlying mechanisms in colorectal cancer have been reported previously (9, 10), the crosstalk between NF-κB, lncRNAs, and mRNAs in colorectal cancer progression remains unknown.

Genomic approaches involving mRNA, miRNA, or lncRNA microarrays coupled with scale-free network analyses have been applied to explore the mechanisms of cancer initiation and progression (11, 12). Weighted gene coexpression network analysis (WGCNA) facilitates the identification of core gene networks based on similar gene-expression patterns across samples (13). The clustered cores or modules identified by WGCNA often represent genes involved in particular biological functions that are either coexpressed or coregulated according to cell type or biological condition (14).

In this study, we used WGCNA to profile differentially expressed lncRNAs and mRNAs in adjacent, adenoma, and colorectal cancer tissues and constructed an lncRNA–transcription factor (TF)–mRNA network. The lncRNA MIR17HG stood out as a key modulator in a feedback loop with NF-κB. Moreover, MIR17HG coordinated with miR-17-5p, thereby negatively

[1]Key Laboratory of Environmental Medicine Engineering, Ministry of Education, School of Public Health, Southeast University, Nanjing, China. [2]Center for New Drug Safety Evaluation and Research, China Pharmaceutical University, Nanjing, China. [3]Department of Maternal, Child and Adolescent Health, School of Public Health, Nanjing Medical University, Nanjing, China. [4]Department of Anatomical, Histological, Forensic Medicine and Orthopedic Science, Sapienza University of Rome, Roma, Italia. [5]Colorectal Cancer Center, Department of General Surgery, Jiangsu Cancer Hospital, Cancer Research Institute, Cancer Hospital of Nanjing Medical University, Nanjing, China. [6]School of Life Sciences, Jiangsu Normal University, Xuzhou, China. [7]Institute for Chemical Carcinogenesis, Guangzhou Medical University, Guangzhou, China.

Note: Supplementary data for this article are available at Cancer Research Online (http://cancerres.aacrjournals.org/).

J. Xu and Q. Meng contributed equally to this article.

Corresponding Author: Rui Chen, Key Laboratory of Environmental Medicine Engineering, Ministry of Education, School of Public Health, Southeast University, 87 Dingjiaqiao, Gulou District, Nanjing 210009, China. Phone: 86-25-83272560; Fax: 86-25-83324322; E-mail: 101011816@seu.edu.cn

Cancer Res 2019;79:4882–95

doi: 10.1158/0008-5472.CAN-18-3880

Published OnlineFirst August 13, 2019; DOI: 10.1158/0008-5472.CAN-18-3880

regulating BLNK expression. In addition, MIR17HG directly bound and upregulated PD-L1, indicating its potential role in immunotherapy. These findings indicated an oncogenic role for MIR17HG in colorectal cancer and elucidated its significance in immunotherapy.

Materials and Methods

The complete details of all reagents and procedures used in this study are provided in the Supplementary Appendix and Supplementary Materials and Methods.

Patients and specimens

All the participants signed written informed consent form before recruitment. The study was conducted in accordance with the Declaration of Helsinki and approved by the Ethics Committee of Southeast University Affiliated Zhongda Hospital.

The tissue samples used for microarray analysis were obtained from 6 colorectal cancer patients and 6 adenoma patients. Detailed clinical information is shown in Supplementary Table S1.

Colorectal cancer and matched adjacent tissues (5 cm from the tumor margin) from 2 independent cohorts were used for tissue microarray (TMA) construction. Two independent cohorts were enrolled in this study between January 2007 and October 2011. In the testing cohort, 376 colorectal cancer patients were enrolled at the Affiliated Hospital of Xuzhou Medical University. In the validation cohort, 431 colorectal cancer patients were enrolled at the Jiangsu Tumor Hospital. All patients were newly diagnosed and histologically confirmed colorectal cancer cases with no preoperative chemo/radiotherapy. Detailed information is presented in Supplementary Table S2. Signed informed consent was provided by each subject before recruitment. The pathologic stage of colorectal cancer was assessed by the 6th edition of the American Joint Committee on Cancer cancer staging manual. All patients were followed up in person or by phone until the time of death or last follow-up (June 2016). The maximum follow-up time was 112.7 months with a median survival time (MST) of 67.1 months.

Fresh colorectal cancer and the corresponding adjacent tissues as well as colorectal adenoma (ADE) tissues were collected at the Jiangsu Tumor Hospital and the Affiliated Hospital of Xuzhou Medical University from 2014 to 2015. Detailed information is presented in Supplementary Tables S3 and S4. The expression levels of the indicated lncRNAs, miRNAs, and mRNAs were detected in these tissues.

WGCNA

A coexpression network for lncRNAs and mRNAs was built using the WGCNA package in R (13). WGCNA provides information about each gene, summary statistics, and module membership (i.e., a measure of how strongly the expression profile of a gene correlates with that of the module) that can be used to screen candidate genes for further functional studies. To construct a scale-free network, Pearson correlation matrix was determined for all gene pairs and transformed into an adjacency matrix using the power function. Next, a weighted network was created. Module is defined as a group of densely interconnected molecules with high topological overlap in the weighted network analysis.

Cell lines and transfection

The cell lines HCT15, HCT116, SW480, SW620, HT29, DLD-1, RKO, and LoVo were obtained from ATCC in 2016. These cells were tested by short tandem repeat analysis, validated to be free of *Mycoplasma*, which were used within 6 months. In addition, the cells were cultured within 25 passages for all experiments. All cell lines were maintained in DMEM (Gibco), 10 % (v/v) fetal bovine serum (Sigma), 100 U/mL penicillin (Gibco), and 100 μg/mL streptomycin (Gibco) at 37°C in 5% CO_2.

Transfection was performed with Lipofectamine 2000 (Invitrogen) or Lipofectamine RNAiMAX (Invitrogen) according to the manufacturer's protocols. The small interfering RNA (siRNA) of the MIR17HG silencer RELA was purchased from Guangzhou RiboBio Co. Ltd.

TMA

Paraffin-embedded blocks of cancer tissue and matched adjacent tissue specimens from the testing and validation cohorts were used for TMA construction at the National Engineering Center for Biochip (Shanghai, China). For each case, 1-mm cores were transferred to a TMA block. The biopsies of adjacent colorectal epithelial tissues were then inserted into the center of each slide with the 4 angles used as negative controls.

Chromatin immunoprecipitation assay

Chromatin immunoprecipitation (ChIP) assay was performed with the EZ-ChIP Chromatin Immunoprecipitation Kit (Millipore). Briefly, cross-linked chromatin DNA was proceeded by sonication into 200 to 500 base pair (bp) fragments. Then, chromatin was immunoprecipitated with the corresponding antibodies. The isolated DNA was assessed by quantitative real-time PCR (qRT-PCR) using SYBR Green Mix.

RNA immunoprecipitation assay

The SW620 cells were cotransfected with MS2 plasmids (Genaray). After 48 hours, the cells were subjected to RNA immunoprecipitation (RIP) assay using the Magna RIP RNA-Binding Protein Immunoprecipitation Kit (Millipore) according to the manufacturer's instructions. The abundance levels of coprecipitated RNAs were detected by qRT-PCR. Total RNA (input controls) and the IgG controls of the corresponding species were assayed simultaneously.

Animals

Mice were housed (5 animals per cage) on corncob bedding with food and water ad libitum, and they were handled according to the guidelines of the Committee on Animal Use and Care of Southeast University.

RELA$^{-/-}$ mouse establishment

In this study, RELA^{fl} (B6.129S1-*Rela*^{tm1Ulkl}/J, Stock No: 024342) mice were purchased from The Jackson Laboratory. PVillin-Cre mice (B6/JNju-Tg(PVillin-Cre)D/Nju), which express Cre recombinase specifically in the intestine, were purchased from Model Animal Research Center of Nanjing University, China. To generate the RELA$^{-/-}$ mice, RELA$^{fl/fl}$ mated with PVillin-Cre transgenic mice to obtain RELA$^{+/-}$ mice. Next, we caged RELA$^{fl/fl}$ and RELA$^{+/-}$ mice to obtain RELA $^{Flox/Flox}$; PVillin-Cre mice, which we called RELA$^{-/-}$ mice here because we only had one type of conditional KO mice in this study.

RELA$^{fl/fl}$ and RELA$^{-/-}$ mice (30 mice per group) were intraperitoneally injected with 10 mg/kg azoxymethane (AOM)

Published OnlineFirst August 13, 2019; DOI: 10.1158/0008-5472.CAN-18-3880

(Sigma). One week later (day 7), all mice were administered 2.5% (w/v) dextran sulfate sodium (DSS; MW: 36,000–50,000; ICN Pharmaceuticals) in drinking water for 3 cycles of 5 days of DSS and 16 days of regular drinking water. Mouse death was monitored. A total of 10 mice per group were sacrificed on day 84 (14 days after the end of the third DSS treatment cycle), then colorectal tumor formation was observed. After sacrifice, 6 of the 10 colon tissues were fixed with 4% paraformaldehyde (PFA), and the remaining 4 were snap frozen in liquid nitrogen. The remaining mice were maintained until day 120. A combined pathologic score ranging from 0 to 6 was used to evaluate DSS-induced colitis (6).

Xenograft assays *in vivo*

Female nude mice (18–20 g) were purchased from the Model Animal Research Center of Nanjing University, China. Nude mice were injected subcutaneously on the dorsal flank with 5×10^6 luciferase-expressing, stably transformed cells suspended in 0.2 mL DMEM. Three weeks after injection, the mice were sacrificed under ether anesthesia. Lung, liver, and xenograft tissues were removed, and luciferase activities were determined on a luminometer (Sirius, Berthold Detection Systems).

Statistical analysis

The χ^2 test was used to evaluate the associations of MIR17HG expression with clinical variables. The Wilcoxon test was used to assess the differences in MIR17HG, BLNK, and RELA staining scores in the TMA. Log-rank test was used to analyze the survival curves. Fisher r-to-z transformation test followed by the Pearson correlation test was used to analyze the correlation. Hazard ratios (HR) and 95%CIs were determined by univariate or multivariate Cox regression analysis with adjustments for age, gender, location (colon or rectum), grade (low or intermediate/high differentiation), and clinical stage (I/II or III/IV). Statistical analysis was performed with SPSS 21.0, with $P < 0.05$ considered statistically significant.

Results

Construction of a lncRNA and mRNA network involved in colorectal cancer progression by WGCNA systemic analysis

The lncRNA and mRNA expression profiles of colorectal cancer, colorectal adenoma, and adjacent tissues ($n = 6$ in each condition) were determined by microarray analysis (Fig. 1A and B). To further assess lncRNA and mRNA coexpression patterns, WGCNA was used to identify genes that played pivotal roles in colorectal cancer development. A total of 27 modules were identified (Fig. 1C), including 10 that were significantly correlated with colorectal cancer progression. In contrast, these modules showed no clear associations with gender, and only some of them were associated with age (Fig. 1D). Wilcoxon test results revealed that module 1 (M1), module 14 (M14), and module 15 (M15) were gradually increased or decreased from adjacent, colorectal adenoma to colorectal cancer tissue samples, with no effects of age and gender observed in the 27 modules (Fig. 1E). Thus, we focused on M1, M14, and M15 in subsequent experiments.

Based upon microarray profiles in these three modules, the heat map (Supplementary Fig. S1A) and differentially expressed genes (DEG) in the modules were analyzed using the Kyoto Encyclopedia of Genes and Genomes (KEGG) database to identify the corresponding biological pathways (Supplementary Fig. S1B). DEGs in both M1 and M14 showed significantly enriched KEGG pathways ($P < 0.05$), including immunity-associated pathways; however, there was no markedly enriched KEGG pathways in M15. Therefore, the emerged mRNAs in M1 and M14 were pooled for sequential analysis, revealing an integrated network of mRNAs and their correlated lncRNAs [fold change (FC) > 1.5] that were involved in immunity-associated pathways (Fig. 1F). Traditionally, the mechanism of competing endogenous RNAs (ceRNA) is used to explore the detailed connections between the targeted lncRNAs and mRNAs. In this study, the complex network was assessed at the transcriptional level. Thus, to further explore key connection nodes in immunity pathways between M1 and M14, we initially constructed a gene-TF regulatory network for M14 in which a subunit of NF-κB, RELA, was identified as the transcription factor with the highest degree (Fig. 1G). Subsequently, bioinformatics analysis suggested that NF-κB, a traditional TF in the immune response, was also transcriptionally related to the M1 immune pathway–involved genes. It turned out that NF-κB transcriptionally regulated 19 mRNAs and was associated with 21 lncRNAs involved in the M1 immune pathway (Fig. 1H). These findings suggested that the cross-talk between immune pathways in M1 and M14 was linked by NF-κB, including a total of 9 lncRNAs and 19 mRNAs (Fig. 1I).

MIR17HG is upregulated in colorectal cancer and transcriptionally activated by NF-κB/RELA

The expression patterns of the 9 lncRNAs involved (Fig. 1I) were validated by qRT-PCR in fresh tumor, adenoma, and adjacent tissues ($n = 96$ per group). The results showed increasing expression patterns for MIR17HG and LINC00460, with gradually decreasing expression levels of XLOC_006495, from adjacent to adenoma, and colorectal cancer tissues (Fig. 2A, left; Supplementary Fig. S1C). Moreover, the expression levels of RELA, the key connection node between M1 and M14, were gradually accumulated from adjacent to adenoma, and colorectal cancer tissues (Fig. 2A, right), which is consistent with the data retrieved from The Cancer Genome Atlas (TCGA; Supplementary Fig. S1D). Finally, according to the above experimental data, the coexpression network constructed in Fig. 1I was reorganized as illustrated in Supplementary Fig. S1E.

To further define the associations of the 3 lncRNA candidates with RELA, knockdown assays were performed using siRNAs. As shown in Fig. 2B, MIR17HG levels were significantly blunted after RELA knockdown in all tested colorectal cancer cell lines. Correspondingly, RELA was also attenuated after MIR17HG ablation in 8 colorectal cancer cell lines. However, this correlational regulation did not occur for LINC00460 and XLOC_006495 (Supplementary Fig. S1F).

Given the importance of RELA in the TF regulatory network, we assessed the role of RELA in colorectal cancer progression using mice models. $RELA^{fl/fl}$ and $RELA^{-/-}$ mice were studied using an azoxymethane-dextran sodium sulfate (AOM-DSS) model. As illustrated in Fig. 2C, colon shortening, which is the macroscopic parameter of colitis severity, was more pronounced in AOM-DSS–treated $RELA^{fl/fl}$ mice compared with $RELA^{-/-}$ mice (4.585 ± 0.549 cm vs. 5.917 ± 0.728 cm). Both $RELA^{fl/fl}$ and $RELA^{-/-}$ mice developed tumors in the middle and distal colons; however, $RELA^{fl/fl}$ mice developed a markedly greater number of tumors, higher tumor formation rate, and shorter overall survival time (Fig. 2C, right; Fig. 2D). Histologic examination consistently showed low- to medium-grade neoplasia in $RELA^{-/-}$ mice

Published OnlineFirst August 13, 2019; DOI: 10.1158/0008-5472.CAN-18-3880

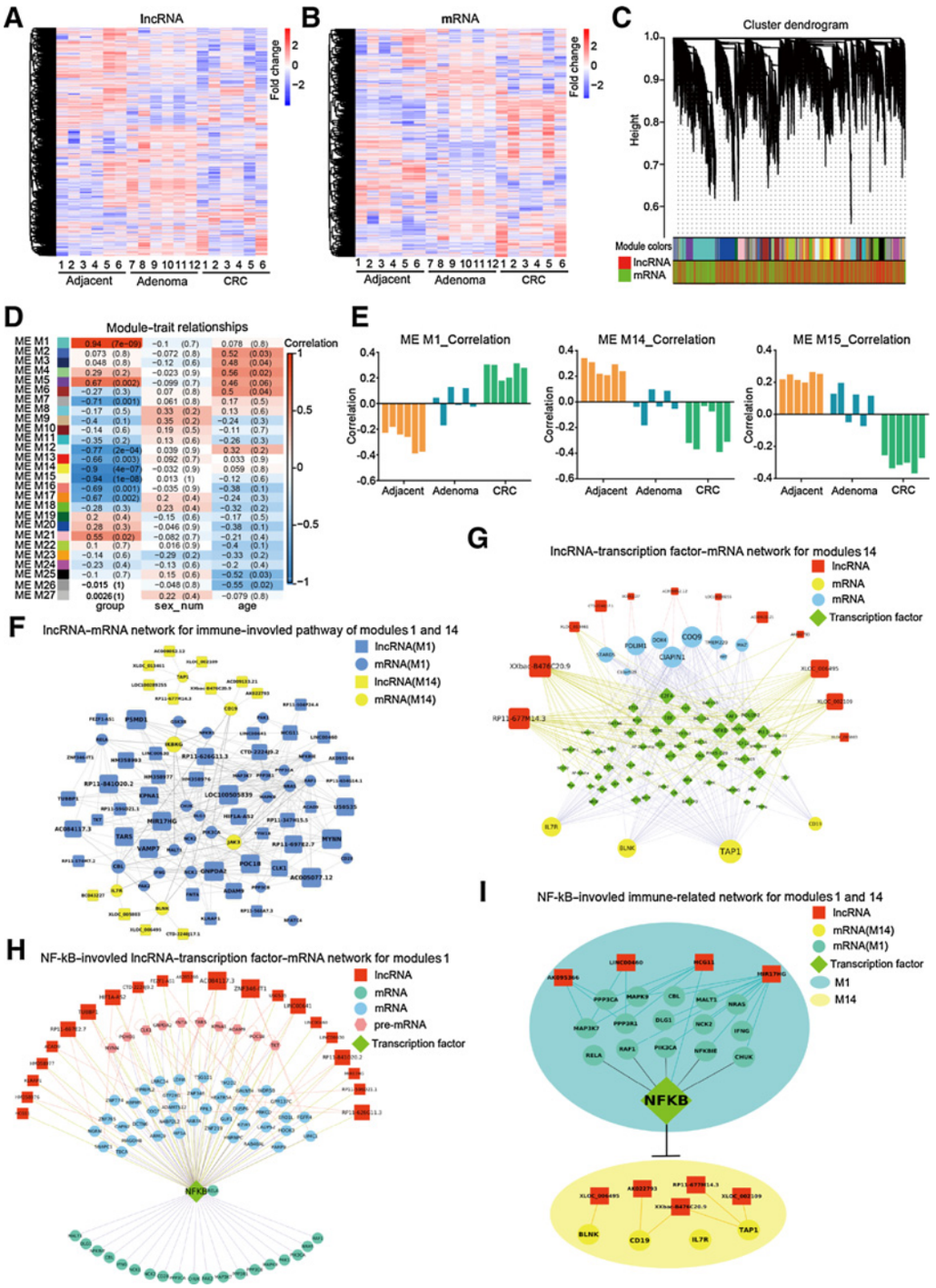

Figure 1.

Construction of the lncRNA and mRNA network involved in colorectal cancer (CRC) progression by WGCNA analysis. **A** and **B,** A total of 6 pairs of colorectal cancer and corresponding adjacent tissues, and 6 adenoma tissue specimens were subjected to lncRNA and mRNA microarray analysis, respectively. Heat maps revealed DEGs (6 biological replicates). **C,** Cluster dendrogram of modules identified by WGCNA of lncRNA and mRNA microarray data. **D,** Associations of modules with clinical characteristics. In each column group, from left to right: adjacent, ADE, and colorectal cancer groups. **E,** A total of three modules (M1, M14, and M15) were found to be significantly correlated with colorectal cancer progression independent from gender and age (Wilcoxon test). **F,** Network of immune-related mRNAs and lncRNAs in M14 and M1. **G,** lncRNA–TF–mRNA network in M14, with NF-κB exhibiting the highest degree. **H,** NF-κB–associated lncRNA–TF–mRNA network in M1. **I,** NF-κB/RELA was predicted as a pivotal component in the coexpression network based on M1 and M14.

Published OnlineFirst August 13, 2019; DOI: 10.1158/0008-5472.CAN-18-3880

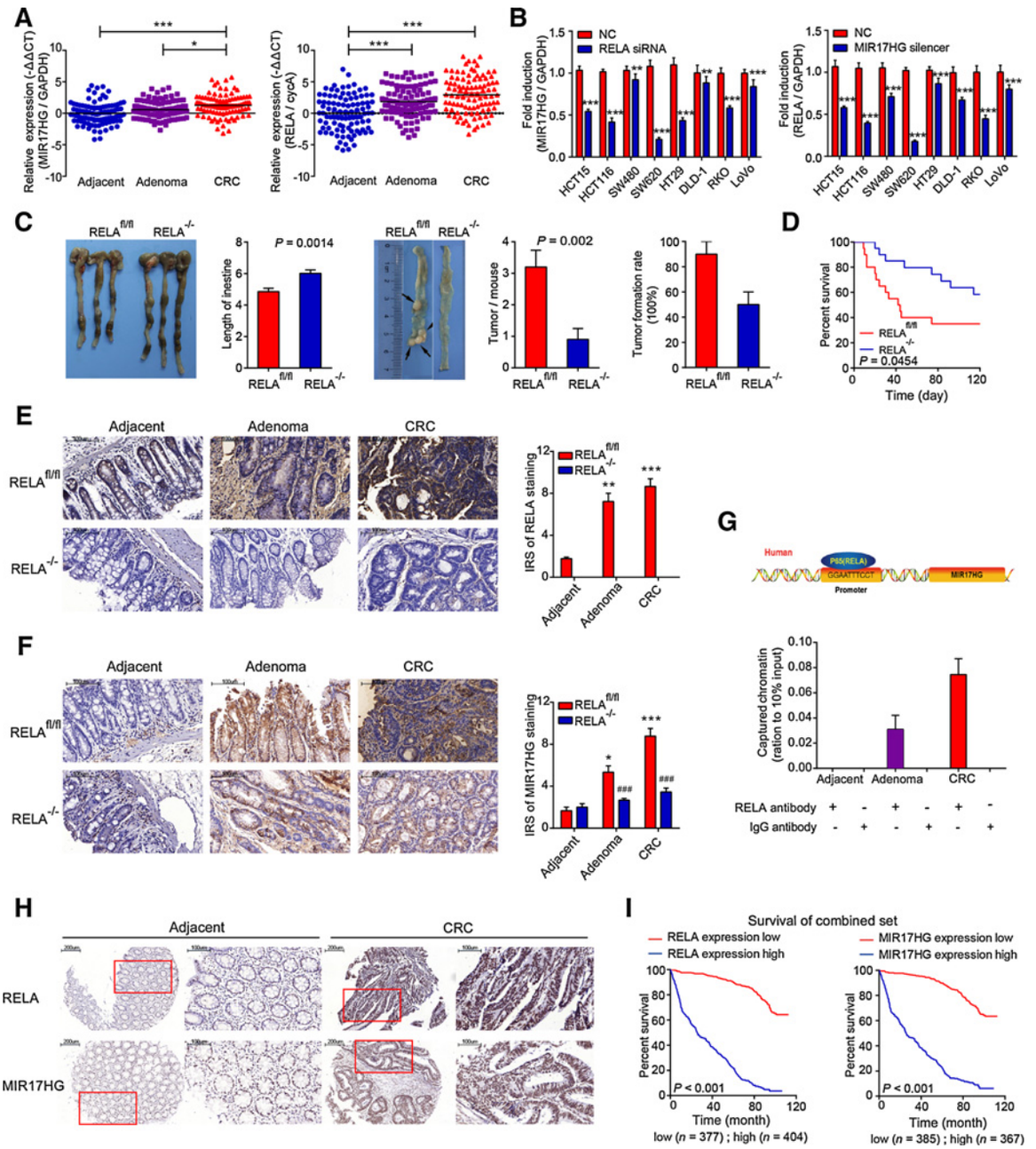

Figure 2.

MIR17HG is accumulated in colorectal cancer (CRC) and transcriptionally activated by NF-κB/RELA. **A,** The expression levels of MIR17HG and RELA in adjacent, adenoma, and colorectal cancer tissues were analyzed by qRT-PCR ($n = 96$ per group; *, $P < 0.05$; ***, $P < 0.001$, one-way ANOVA). **B,** Left, colorectal cancer cell lines were treated with RELA siRNA or the negative control siRNA. The expression levels of MIR17HG in the indicated cells were determined by qRT-PCR. Right, colorectal cancer cell lines were treated with the MIR17HG silencer or the negative control. The expression levels of RELA in the indicated cells were determined by qRT-PCR ($n = 6$; **, $P < 0.01$; ***, $P < 0.001$, two-tailed t test). **C,** Representative images of colons from $RELA^{fl/fl}$ and $RELA^{-/-}$ mice administered the AOM-DSS regimen ($n = 10$ per group; two-tailed t test). Macroscopic images of intestines, intestine lengths, tumor counts per mouse, and tumor formation rates. **D,** The overall survival of the indicated mice was assessed using the KM method. P values were calculated by the log-rank test ($n = 20$). **E** and **F,** IHC and ISH were applied to detect RELA and MIR17HG expression, respectively, in colorectal tissues from mice with the indicated treatments. The representative images and calculated IRS are shown ($n = 9$; *, $P < 0.05$; **, $P < 0.01$; ***, $P < 0.001$, compared with adjacent tissue in $RELA^{fl/fl}$ mice, Kruskal–Wallis test followed by the Dunn multiple comparison test; ##, $P < 0.001$, compared with $RELA^{fl/fl}$ of each subgroup, two-tailed t test). **G,** Top, a schematic diagram depicting the binding site of RELA in the promoter region of MIR17HG. Bottom, the binding affinity for MIR17HG and RELA was detected by ChIP assays. **H,** The levels of RELA and MIR17HG in TMA were evaluated by IHC and ISH, respectively. The representative staining images are shown. The scale bar is marked in each image. **I,** KM curves depicting the overall survival of colorectal cancer patients in the combined cohort that was based upon tumoral RELA and MIR17HG levels, respectively. P values were calculated by the log-rank test.

Published OnlineFirst August 13, 2019; DOI: 10.1158/0008-5472.CAN-18-3880

compared with medium- to high-grade in $RELA^{fl/fl}$ mice (Supplementary Fig. S2A). Similarly, RELA levels displayed an increasing trend from adjacent to adenoma, and colorectal cancer tissues in $RELA^{fl/fl}$ mice, but not in $RELA^{-/-}$ mice (Fig. 2E).

To seek the sequential events involved in the RELA-related colorectal cancer carcinogenesis, MIR17HG expression levels were detected in $RELA^{fl/fl}$ compared with $RELA^{-/-}$ mice in the AOM-DSS model. *In situ* hybridization (ISH) demonstrated that MIR17HG exhibited an increasing trend from adjacent to adenoma, and colorectal cancer tissues in $RELA^{fl/fl}$ mice, but not in $RELA^{-/-}$ mice (Fig. 2F). Collectively, these results suggested that RELA transcriptionally regulated MIR17HG in murine colorectal tumorigenesis. In using ChIP assays to further assess the biological relationship between MIR17HG and RELA, the RELA protein was found to directly bind to the specific motif in the MIR17HG promoter region (Fig. 2G).

In addition, the MIR17HG expression pattern positively correlated with the RELA mRNA levels in colorectal cancer patients ($n = 96$; Supplementary Fig. S2B). Furthermore, based upon the ISH analysis from TMA with 5 years survival information, the data showed that the relative expression levels of MIR17HG and RELA were dramatically accumulated in colorectal cancer tumor tissues compared with adjacent tissues not only in the testing but also in the validation cohorts (Fig. 2H; Supplementary Fig. S2C). Moreover, Kaplan–Meier (KM) analysis showed that patients with high expression of both RELA and MIR17HG gained a significantly shorter overall survival time than those with low levels (Fig. 2I; Supplementary Fig. S2D). Taken together, these findings indicated that MIR17HG was transcriptionally activated by NF-κB/RELA. Therefore, further assessment of the MIR17HG function in colorectal cancer was important.

MIR17HG promotes colorectal cancer growth and metastasis through suppressing BLNK expression binding with miR-17-5p

Typically, MIR17HG is the miR-17-92 cluster host gene, which has been reported to promote carcinogenesis in different tumors (15, 16). BLNK, previously identified in the network of M14, was predicted to be targeted by the miR-17-92 cluster in the miRBase and TargetScan databases (Fig. 3A). Data retrieved from TCGA showed significantly higher expression levels of the miR-17-92 cluster (miR-17-5p, miR-17-3p, and miR-19b-1-5p) in colorectal cancer tissues compared with in normal ones (Supplementary Fig. S3A). Only miR-17-5p was differentially expressed among adjacent, adenoma, and colorectal cancer tissue samples among these three miRNAs as quantified using qRT-PCR (Fig. 3B, left). Subsequently, the role of miR-17-5p in the tumorigenesis of colorectal cancer was explored. SW620 and HCT116 cells lost colony formation, migration, and invasion capabilities, as well as tumor formation and metastasis lacking the miR-17-5p (Supplementary Fig. S3B–S3E). As shown in Supplementary Fig. S3F and S3G, miR-17-5p augmentation in colorectal cancer tumor compared with adjacent tissues by TMA and KM analysis. Clearly, the mean overall survival time in patients with relatively high miR-17-5p expression was decreased significantly in the testing and/or validation cohorts. Moreover, as the predicted target gene for the miR-17-92 cluster, BLNK displayed a reverse trend compared with miR-17-5p in tissues (Fig. 3B, right). Consistently, data retrieved from TCGA suggested significantly lower expression levels of BLNK in colorectal cancer compared with that of normal tissues (Supplementary Fig. S4A).

To verify BLNK regulation by miR-17-5p, luciferase reporter assays were performed in SW620 and HCT116 cells. The overexpression of miR-17-5p resulted in the blunting of the luciferase activity of wild-type but not the mutated BLNK 3′UTR, which suggested that miR-17-5p directly regulated BLNK expression by binding the BLNK 3′UTR (Fig. 3C). We then tested if MIR17HG regulated BLNK through miR-17-5p. Our data showed that the mRNA levels of BLNK were increased by miR-17-5p or MIR17HG individual knockdown and blunted with either miR-17-5p or MIR17HG overexpression (Supplementary Fig. S4B). Furthermore, the co-overexpression of MIR17HG and miR-17-5p decreased BLNK expression, and the double knockdown of MIR17HG and miR-17-5p showed the opposite effect (Fig. 3D). Notably, BLNK was upregulated after MIR17HG overexpression while miR-17-5p was knocked down. In contrast, BLNK was decreased after MIR17HG knockdown combined with miR-17-5p overexpression (Fig. 3E), which suggested that MIR17HG might be an upstream regulator of miR-17-5p and BLNK. In addition, miR-17-5p expression was negatively correlated to BLNK mRNA levels in colorectal cancer, which was similar to the relationship between MIR17HG and BLNK ($n = 96$; Supplementary Fig. S4C). Accordingly, we confirmed the MIR17HG/miR-17-5p/BLNK molecular cascade in colorectal cells (Fig. 3F).

The suppression of BLNK has been reported in different tumor tissues (17–19); however, the role of BLNK in colorectal cancer tumorigenesis remains unclear. Here, SW620 and HCT116 cells were stably transfected with BLNK shRNA and a nontargeting shRNA control labeled with firefly luciferase. Blunt of BLNK strikingly accumulated colony formation, migration, and invasion abilities in both SW620 and HCT116 cells (Fig. 3G; Supplementary Fig. S4D). In agreement, *in vivo* data showed that increased tumor volumes were observed in nude mice lacking BLNK. The same pattern was observed with liver and lung luciferase biochemical measurements, with markedly promoted liver and lung metastasis in mice carrying flank tumors expressing low levels of BLNK (Fig. 3H; Supplementary Fig. S4E). Moreover, TMA analysis showed that BLNK expression levels were reduced dramatically in colorectal cancer tumor tissues compared with adjacent samples (Fig. 3I; Supplementary Fig. S4F). Consistently, KM analysis revealed that the mean overall survival time was significantly decreased in patients with relatively low BLNK expression (Fig. 3J; Supplementary Fig. S4G).

RELA attenuates BLNK expression through activating MIR17HG

Given that MIR17HG and the miR-17-92 cluster are transcribed from the same locus, and that MIR17HG was transcriptionally upregulated by RELA, we evaluated whether RELA could transcriptionally activate the miR-17-92 cluster. Therefore, we detected miR-17-3p, miR-19b-1-5p, and miR-17-5p expression levels in $RELA^{fl/fl}$ and $RELA^{-/-}$ mice by ISH assay. The results showed that miR-17-5p was blunted only in colorectal adenoma and cancer tissues from $RELA^{-/-}$ mice, but not in the $RELA^{fl/fl}$ mice (Fig. 4A; Supplementary Fig. S5A and S5B).

Based upon the previous findings on the two regulatory cascades of MIR17HG/miR-17-5p/BLNK and RELA/miR-17-5p in the colorectal cancer carcinogenesis, we next assessed if BLNK was directly regulated by RELA. Interestingly, compared with the miR-17-5p results, the opposite was observed for BLNK as protein levels were instead gradually reduced from adjacent to adenoma,

Published OnlineFirst August 13, 2019; DOI: 10.1158/0008-5472.CAN-18-3880

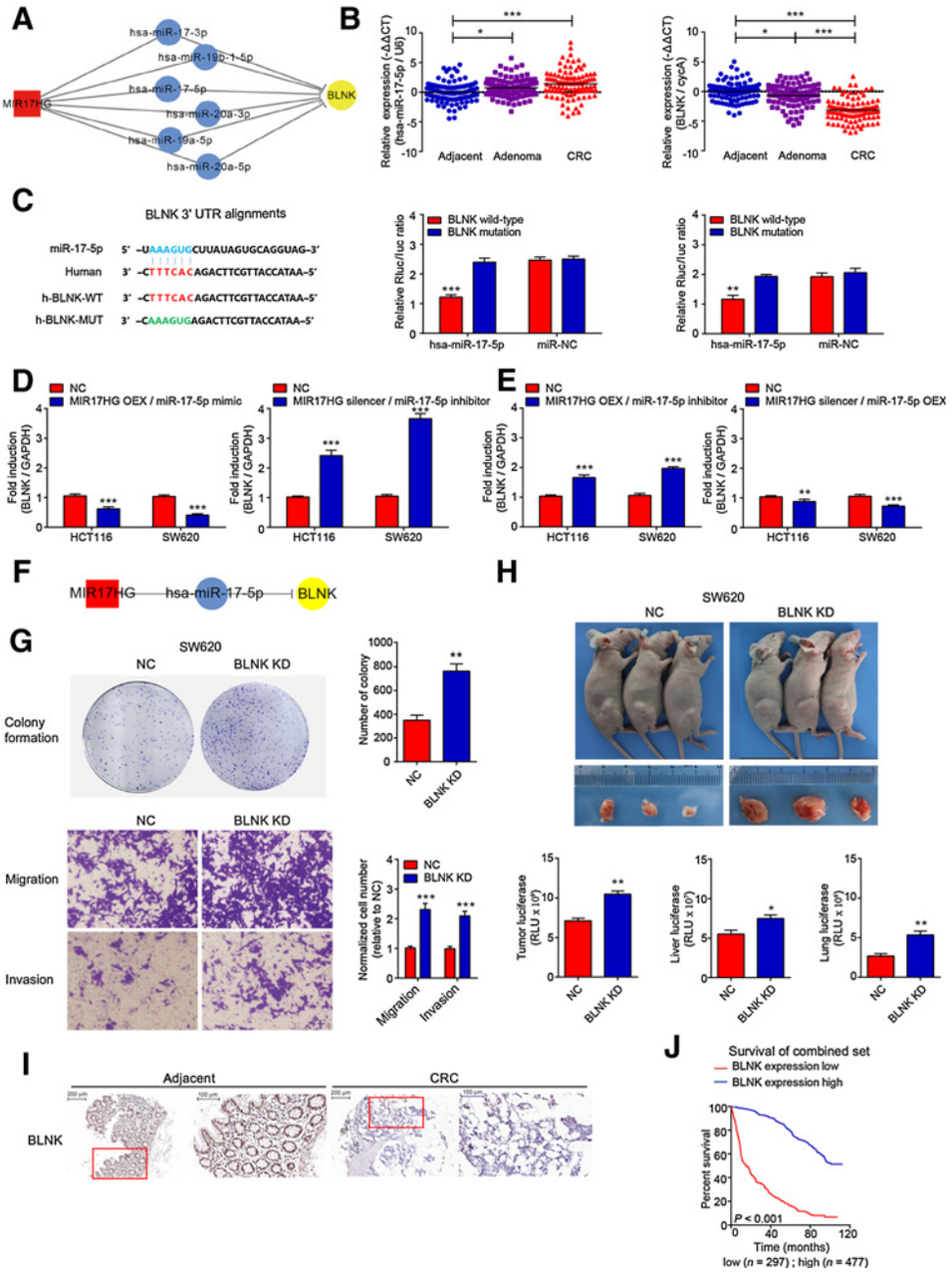

Figure 3.

MIR17HG promotes colorectal cancer (CRC) growth and metastasis through binding with miR-17-5 to suppress BLNK. **A,** MIR17HG was predicted to repress BLNK through the miR-17-92 cluster. **B,** The expression levels of miR-17-5p and BLNK in adjacent, adenoma, and colorectal cancer tissues were analyzed by qRT-PCR ($n = 96$ per group; *, $P < 0.05$; ***, $P < 0.001$, one-way ANOVA). **C,** Schematic diagram of the construction of BLNK WT and mutant luciferase reporter plasmids. SW620 and HCT116 cells expressing BLNK WT and mutant luciferase reporter plasmids were incubated with miR-17-5p mimics and the negative control. The relative luciferase activities of the indicated cells are shown. Data are presented as the ratio of *Renilla* luciferase activity to firefly luciferase activity ($n = 3$; **, $P < 0.01$; ***, $P < 0.001$, compared with BLNK mutation and miR-NC–treated cells, ANOVA followed by Tukey multiple comparison test). **D** and **E,** The expression levels of BLNK in cells with the indicated treatments were determined by qRT-PCR ($n = 6$; **, $P < 0.01$; ***, $P < 0.001$, compared with NC-treated cells within each group, two-tailed *t* test). **F,** Schematic diagram depicting the MIR17HG–miR-17-5p–BLNK axis. **G,** Top, SW620 with the indicated treatments was subjected to colony formation assay ($n = 6$; **, $P < 0.01$, compared with NC, two-tailed *t* test). Bottom, SW620 with the indicated treatments was subjected to migration and invasion assays ($n = 3$; ***, $P < 0.001$, compared with NC, two-tailed *t* test). **H,** Top, SW620 with the indicated treatments were subcutaneously injected into nude mice ($n = 6$). The representative images of xenografts are shown. Bottom, subcutaneous tumors, liver, and lung tissues of the indicated mice were harvested, and luciferase activities were analyzed ($n = 6$; *, $P < 0.05$; **, $P < 0.01$, compared with NC, two-tailed *t* test). **I,** The protein levels of BLNK in TMA were evaluated by IHC. The representative staining images are shown. **J,** KM curves depicting the overall survival of colorectal cancer patients in the combined cohort, based upon tumoral BLNK levels. *P* values were calculated by the log-rank test.

Published OnlineFirst August 13, 2019; DOI: 10.1158/0008-5472.CAN-18-3880

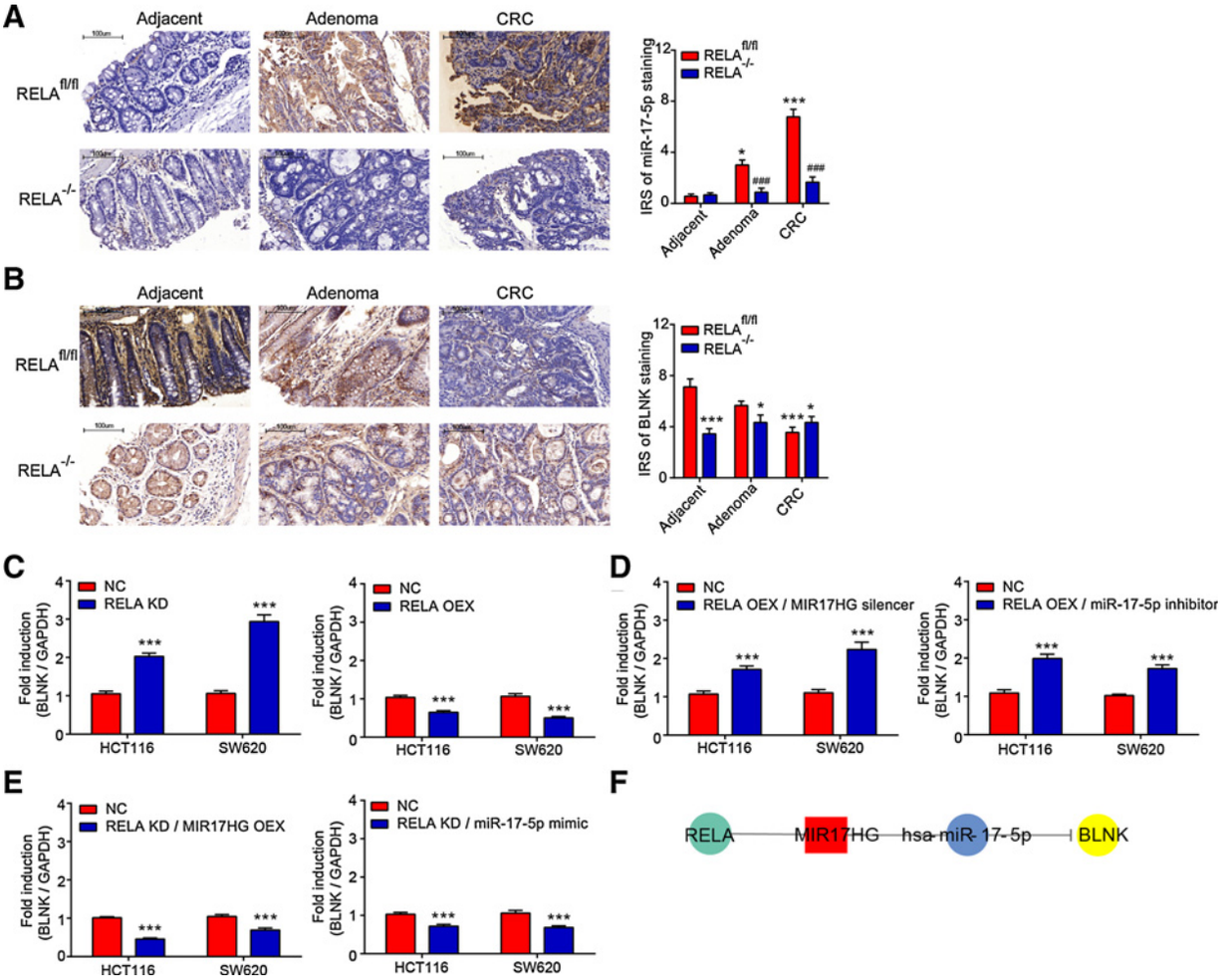

Figure 4.

The molecular pathway RELA/MIR17HG/miR-17-5p/BLNK is involved in colorectal cancer (CRC) tumorigenesis. **A** and **B,** ISH and IHC were applied to detect miR-17-5p and BLNK expression, respectively, in colorectal tissues from the indicated mice. The representative images and calculated scores are shown ($n = 9$; *, $P < 0.05$; ***, $P < 0.001$, compared with adjacent tissue in RELA$^{fl/fl}$ mice, Kruskal–Wallis test followed by the Dunn multiple comparison test; $^{###}$, $P < 0.001$, compared with RELA$^{fl/fl}$ of each subgroup, two-tailed *t* test). The scale bar is marked in each image. **C–E,** The expression levels of BLNK in cells with the indicated treatments were determined by qRT-PCR ($n = 6$; ***, $P < 0.001$, compared with NC-treated cells within each group, two-tailed *t* test). **F,** Schematic diagram depicting the RELA–MIR17HG–miR-17-5p–BLNK axis.

and colorectal cancer tissues in RELA$^{fl/fl}$ mice, with no differences identified due to the lack of RELA (Fig. 4B). Furthermore, we confirmed the specific regulation pattern of BLNK by RELA in colorectal cancer cell lines. Both the BLNK augmentation of RELA knockdown and BLNK attenuation of RELA overexpression were clearly observed (Fig. 4C). Additionally, the *in vitro* modulation of BLNK expression by RELA indicated that the latter was upstream of MIR17HG in the molecular cascade (Fig. 4D and E). Taken together, these data revealed the molecular pathway of RELA/MIR17HG/miR-17-5p/BLNK in colorectal cancer tumorigenesis (Fig. 4F).

To further clarify these molecular pathway events of MIR17HG, RELA, miR-17-5p, and BLNK on the clinicopathologic characteristics of colorectal cancer patients, multivariate regression analysis was performed in the testing and/or validation cohorts. As shown in Table 1, high expression levels of MIR17HG, RELA, and miR-17-5p, advanced tumor stage, and advanced age were associated with shorter survival in all cohorts. Meanwhile, BLNK expression appeared to be a positive prognostic factor in colorectal cancer patients. Considering that the expression patterns of MIR17HG and miR-17-5p displayed a strong consistency, we reassessed the correlation between their expression levels in combination and prognosis in colorectal cancer patients. The results suggested that survival time in patients with a high expression of either MIR17HG or miR-17-5p was between those of patients with MIR17HG plus miR-17-5p at high levels and the ones expressing low amounts of MIR17HG plus miR-17-5p (Supplementary Fig. S5C).

MIR17HG accumulates RELA expression by sponging miR-375

lncRNAs work as ceRNAs by competitively sponging miRNAs, resulting in the liberation of target mRNAs (20–22). Because WGCNA analysis indicated that MIR17HG potentially activated RELA in M1, we hypothesized that MIR17HG regulated RELA

Published OnlineFirst August 13, 2019; DOI: 10.1158/0008-5472.CAN-18-3880

Table 1. Multivariate Cox regression analysis of MIR17HG expression and selected clinicopathologic variables with colorectal cancer survival

	Testing cohort ($n = 299$)		Validation cohort ($n = 369$)		Combine cohort ($n = 668$)	
Variables	**Adjusted HR (95% CI)[a]**	***P*[a]**	**Adjusted HR (95% CI)[a]**	***P*[a]**	**Adjusted HR (95% CI)[a]**	***P*[a]**
Age (>55 vs. ≤55)	1.37 (1.03–1.82)	0.0286	1.68 (1.27–2.24)	0.0003	1.55 (1.27–1.89)	<0.0001
Gender (females vs. males)	0.92 (0.69–1.23)	0.5701	0.91 (0.68–1.21)	0.4939	0.92 (0.75–1.13)	0.4249
Location (rectal vs. colon)	0.89 (0.67–1.17)	0.4022	0.83 (0.63–1.09)	0.1784	0.86 (0.71–1.05)	0.1370
Grade (intermediate/high vs. low)	0.82 (0.62–1.10)	0.1877	0.85 (0.64–1.14)	0.2735	0.84 (0.69–1.03)	0.1014
TNM (III/IV vs. I/II)	5.00 (3.68–6.79)	<0.0001	5.74 (4.26–7.73)	<0.0001	5.43 (4.39–6.72)	<0.0001
MIR17HG (high vs. low)	4.99 (3.43–7.27)	<0.0001	8.99 (6.25–12.94)	<0.0001	6.34 (4.92–8.16)	<0.0001
BLNK (high vs. low)	0.26 (0.19–0.35)	<0.0001	0.08 (0.06–0.12)	<0.0001	0.17 (0.14–0.21)	<0.0001
RELA (high vs. low)	6.80 (4.61–10.04)	<0.0001	14.11 (9.39–21.21)	<0.0001	9.52 (7.23–12.53)	<0.0001
miR-17-5p (high vs. low)	8.82 (6.07–12.82)	<0.0001	9.47 (6.40–14.01)	<0.0001	8.03 (6.22–10.38)	<0.0001
MIR17HG/miR-17-5p (one high vs. both low)	5.91 (3.98–8.78)	<0.0001	9.92 (6.75–14.57)	<0.0001	7.25 (5.56–9.47)	<0.0001
MIR17HG/miR-17-5p (both high vs. both low)	62.62 (26.34–148.86)	<0.0001	28.68 (17.11–48.09)	<0.0001	31.69 (21.06–47.70)	<0.0001

[a]Adjusted for age, gender, location (rectum or colon), grade (intermediate/high vs. low), and clinical stage (III/IV vs. I/II).

MALT1, NFKBIE, PPP3R1, MAP3K7, and CBL through sponging miRNAs, which blunt them on the 3′UTR. Indeed, two miRNAs, miR-375 and miR-2116-5p, were predicted to be sponged by MIR17HG via miRBase and TargetScan database analyses (Fig. 5A). To determine if MIR17HG bound to the endogenous miR-375/miR-2116-5p, MS2-based RIP assays were performed. The results showed that MIR17HG was markedly enriched for miR-375 compared with miR-2116-5p, but not the MIR17HG with mutated miR-375 targeting sites (Fig. 5B). Interestingly, the expression levels of miR-375 in human adjacent, adenoma, and tumor tissues were not significantly altered (Fig. 5C), which means that miR-375 only served as a scaffold to connect MIR17HG and activated mRNAs.

As a proof of concept, the luciferase reporter assay was performed first to confirm RELA, MALT1, NFKBIE, PPP3R1, MAP3K7, and CBL regulation by miR-375. Except for CBL, luciferase activities were attenuated after cell cotransfection with miR-375 and wild-types of RELA, MALT1, NFKBIE, PPP3R1, and MAP3K7 3′UTR, but not the mutant variants, indicating that miR-375 directly targeted these 5 genes (Fig. 5D; Supplementary Fig. S6A). Furthermore, the expression levels of MALT1, NFKBIE, PPP3R1, MAP3K7, and RELA all displayed a significant trend of increasing expression from adjacent to adenoma, and colorectal cancer tissues, corroborating the data retrieved from TCGA (Fig. 2A; Supplementary Figs. S1D and S6B). Moreover, correlation analysis showed that MIR17HG was significantly associated with RELA, MALT1, NFKBIE, PPP3R1, and MAP3K7 mRNA levels in colorectal cancer (Supplementary Figs. S2B and S6B). These findings suggested that MIR17HG activated RELA, MALT1, NFKBIE, PPP3R1, and MAP3K7 in colorectal cancer through the ceRNA mechanism on miR-375.

MIR17HG plays an oncogenic role in colorectal cancer tumorigenesis through building a positive feedback loop with RELA

Because RELA was involved in this regulatory network of ceRNAs, we further assessed RELA regulation by MIR17HG with or without miR-375. The results showed that RELA expression levels were elevated after MIR17HG overexpression (Fig. 5E, left). Consistently, results were observed after MIR17HG overexpression + miR-375 suppression in cells (Fig. 5E, right). Notably, compared with MIR17HG overexpression + miR-375–negative control, the expression level of RELA with MIR17HG overexpression + miR-375 overexpression was significantly inhibited in HCT116 and SW620 cells (Fig. 5F), suggesting the ability of MIR17HG to sponge miR-375 regulate expression of RELA. As previously demonstrated, RELA transcriptionally regulated MIR17HG expression (Fig. 2G). Combined with the current findings, these results indicated a positive feedback loop between MIR17HG and RELA in colorectal cancer tumorigenesis (Fig. 5G).

Taken together, MIR17HG not only inhibited BLNK expression through its cluster member miR-17-5p in colorectal cancer, but also formed a positive feedback loop with RELA. Accordingly, we further assessed the role of MIR17HG in colorectal cancer tumorigenesis. As shown in Fig. 2A, MIR17HG was upregulated in colorectal cancer compared with adjacent and adenoma tissues. To evaluate the oncogenic properties of MIR17HG in colorectal cancer, SW620 and HCT116 cells were transfected with MIR17HG shRNA and a nontargeting shRNA control labeled with firefly luciferase. *In vitro* assays indicated that MIR17HG knockdown in SW620 and HCT116 cells resulted in significantly decreased colony formation, migration, and invasion abilities (Fig. 5H and I). MIR17HG knockdown markedly reduced tumor volumes, the lung and liver metastasis potential after cells were subcutaneously injected into the hind limb of nude mice (Fig. 5J and K). In summary, these data demonstrated that MIR17HG played an oncogenic role in colorectal cancer tumorigenesis.

MIR17HG acts as a potential immunotherapeutic target in colorectal cancer by binding to PD-L1 directly

Given its importance in colorectal cancer immunity-related progression and prognosis, the potential role of MIR17HG in immunotherapy was further evaluated. As shown in Fig. 6A, the interaction of MIR17HG and several established immunotherapeutic targets, including programmed cell death ligand 1 (PD-L1), programmed cell death ligand 2 (PD-L2), T-cell immunoglobulin and mucin-domain containing-3 (TIM-3), and cytotoxic T-lymphocyte-associated antigen 4 (CTLA-4), was evaluated by RNA pulldown assay. Results showed that PD-L1 was bound with MIR17HG in both SW620 and HCT116 cells, indicating the binding between MIR17HG and PD-L1.

As reported, PD-L1 binding the PD-1 transmembrane receptor is considered to regulate T-cell activation and immune responses, which achieved great success in immunotherapy (23, 24). As shown in Supplementary Fig. S7, the mRNA expression levels of PD-L1 in HCT116 and SW620 cells were indistinguishable from control, following either MIR17HG overexpression or knockdown. However, WB assay suggested increased PD-L1 expression following MIR17HG overexpression and decreased PD-L1 expression following MIR17HG knockdown in HCT116 and SW620

Published OnlineFirst August 13, 2019; DOI: 10.1158/0008-5472.CAN-18-3880

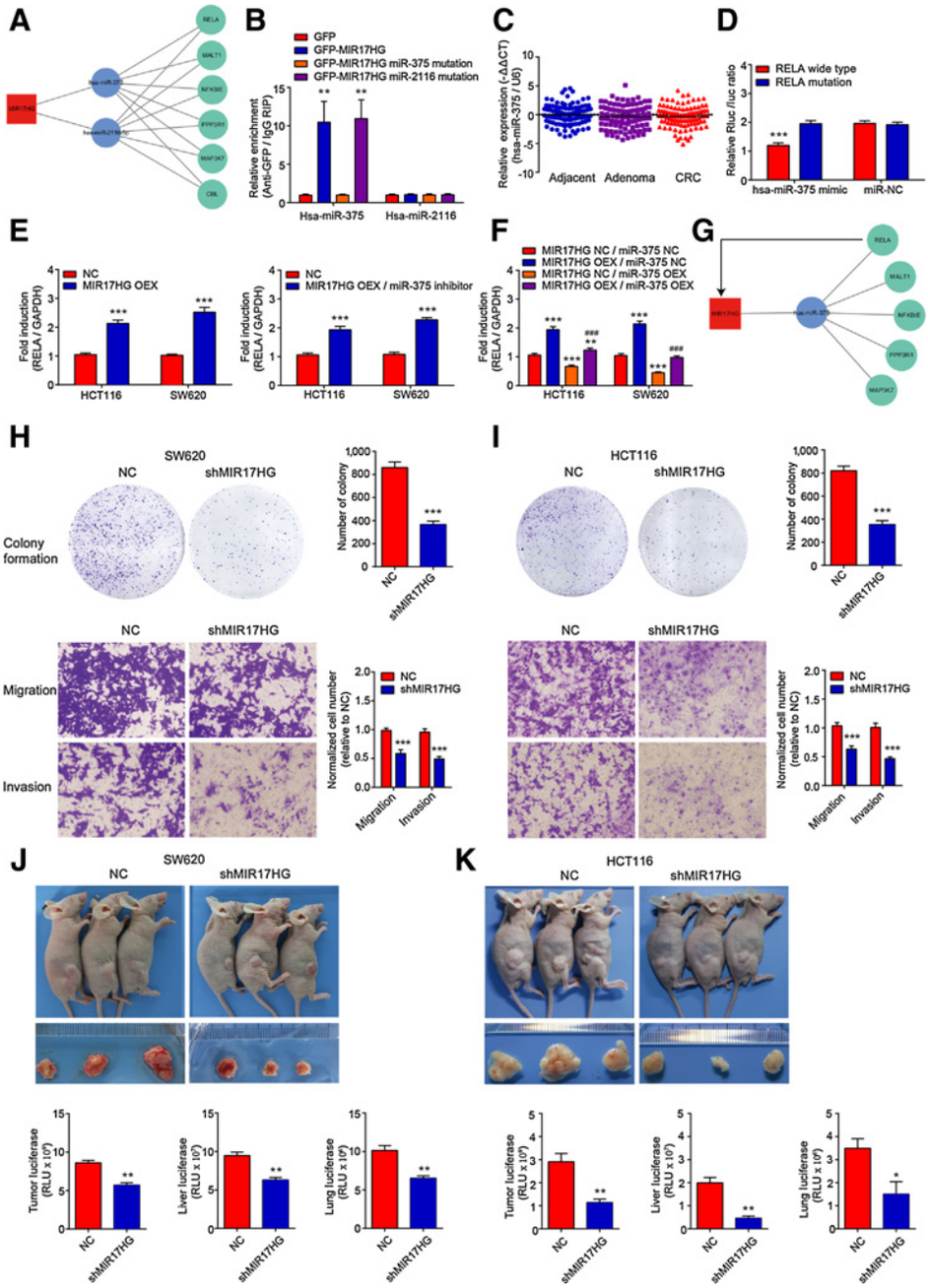

Figure 5.

MIR17HG plays an oncogenic role in colorectal cancer (CRC) tumorigenesis through the positive feedback loop of MIR17HG/RELA by sponging miR-375. **A,** Bioinformatics analysis suggested that MIR17HG might be a ceRNA that is sponging miRNAs. **B,** RIP qRT-PCR detection of the indicated RNAs retrieved by GFP antibodies in SW620 with the indicated treatments ($n = 3$; **, $P < 0.01$, compared with GFP transfected cells within each group, ANOVA followed by the Tukey multiple comparison test). **C,** The expression levels of miR-375 in adjacent, adenoma, and colorectal cancer tissues were determined by qRT-PCR ($n = 96$ per group, one-way ANOVA). **D,** Luciferase activities in cells with the indicated treatments ($n = 3$, ***, $P < 0.001$, ANOVA followed by the Tukey multiple comparison test). **E,** The expression levels of RELA in the indicated cells were determined by qRT-PCR ($n = 6$; ***, $P < 0.001$, compared with NC-treated cells within each group, two-tailed t test). **F,** The expression levels of RELA in the indicated cells were determined by qRT-PCR ($n = 6$; **, $P < 0.01$; ***, $P < 0.001$, compared with NC-treated cells within each group; $^{###}$, $P < 0.001$, co-overexpression compared with MIR17HG OEX/miR-375 NC within each group, two-tailed t test). **G,** A schematic diagram of the MIR17HG-involved ceRNA network. **H** and **I,** SW620 and HCT116 cells with the indicated treatments were subjected to colony formation assay ($n = 6$; ***, $P < 0.001$, compared with NC, two-tailed t test) as well as migration and invasion assays ($n = 3$; ***, $P < 0.001$, compared with NC, two-tailed t test). **J** and **K,** SW620 and HCT116 cells with the indicated treatments were subcutaneously injected into nude mice. The representative images of xenografts are shown. Subcutaneous tumors, liver and lung tissues of the indicated mice were harvested, and luciferase activities were analyzed ($n = 6$; *, $P < 0.05$; **, $P < 0.01$, compared with NC, two-tailed t test).

Published OnlineFirst August 13, 2019; DOI: 10.1158/0008-5472.CAN-18-3880

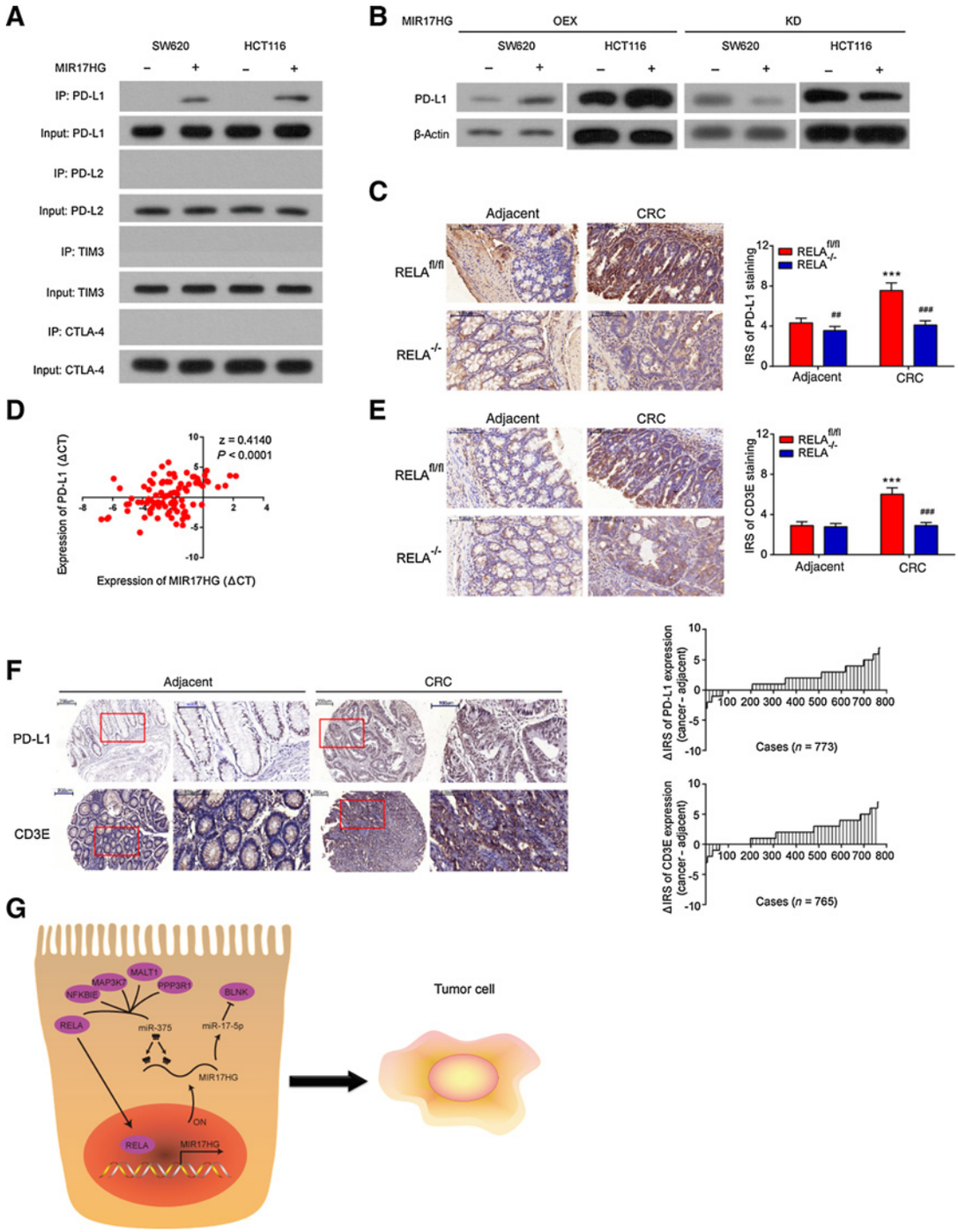

Figure 6.

MIR17HG binds directly to PD-L1, making it a potential immunotherapeutic target for colorectal cancer (CRC). **A,** RNA pulldown assay suggested binding of MIR17HG to PD-L1. **B,** Western blot was used to detect the protein levels of PD-L1 in the indicated cells. **C,** IHC was applied to detect PD-L1 expression in murine tissues with the indicated treatments. The representative images and calculated IRS are shown ($n = 9$; ***, $P < 0.001$, compared with adjacent tissue in RELA$^{fl/fl}$ mice; $^{\#\#}$, $P < 0.01$; $^{\#\#\#}$, $P < 0.001$, compared with RELA$^{fl/fl}$ of each subgroup, two-tailed t test). **D,** Correlation between MIR17HG and PD-L1 expression levels in colorectal cancer tissues ($n = 96$, Fisher r-to-z transformation test followed by the Pearson correlation test). **E,** The levels of CD3E in murine tissues were evaluated by IHC analysis, and the representative staining images and the calculated IRS are shown ($n = 9$; ***, $P < 0.001$, compared with adjacent tissues from RELA$^{fl/fl}$ mice; $^{\#\#\#}$, $P < 0.001$, compared with RELA$^{fl/fl}$ of each subgroup, two-tailed t test). **F,** The levels of PD-L1 and CD3E in TMA were evaluated by IHC, and the staining score differences between colorectal cancer lesions and adjacent tissues (cancer – adjacent) are shown. The scale bar is marked in each image. **G,** The systemic molecular pathway of MIR17HG-mediated tumorigenesis.

Published OnlineFirst August 13, 2019; DOI: 10.1158/0008-5472.CAN-18-3880

cells (Fig. 6B). lncRNA could directly bind to protein and increase the stability of protein without regulation of mRNA levels (23). Therefore, we speculate that MIR17HG regulates expression of PD-L1 on the protein level, but not on the mRNA level. IHC staining suggested significantly lower expression levels of PD-L1 in tumor tissues formed by subcutaneous injection of shMIR17HG-treated SW620 or HCT116 cells, compared with NC-treated control (Supplementary Fig. S8A and S8B). Furthermore, IHC analysis demonstrated that PD-L1 expression levels were significantly higher in tumor tissue than in adjacent normal tissue in $RELA^{fl/fl}$, but not in $RELA^{-/-}$ murine intestine (Fig. 6C), which exhibited the same expression trend as MIR17HG in murine tissues (shown in Fig. 2F). Additionally, correlation analysis documented that levels of PD-L1 and MIR17HG were positively correlated in colorectal cancer tissues (Fig. 6D). Moreover, CD3E, the component of the T-cell receptor–CD3 complex, is required for T-cell activation in immune therapy (24, 25). IHC staining of mice specimens showed that much more CD3E-positive T cells were infiltrated from adjacent to colorectal cancer tissues in $RELA^{fl/fl}$ mice (Fig. 6E). Subsequent TMA analysis confirmed the higher expression levels of PD-L1 and CD3E in colorectal cancer than adjacent tissues (Fig. 6F). Hereby, MIR17HG might be a potential immunotherapeutic target in colorectal cancer.

Overall, our study demonstrated that the lncRNA MIR17HG promoted colorectal cancer tumorigenesis and progression by upregulating RELA in the positive feedback manner. In addition, MIR17HG, the primary precursor for miR-17-5p, suppressed the expression of its target gene BLNK. Furthermore, MIR17HG directly binds to PD-L1, thereby elevating PD-L1 levels in colorectal cancer. Hence, MIR17HG exerted pleiotropic oncogenic effects in colorectal cancer and might serve as a promising immunotherapeutic target (Fig. 6G).

Discussion

Colorectal cancer is one of the most important malignancies worldwide accompanied by a high rate of morbidity and mortality (26). Although the survival of colorectal cancer patients has significantly progressed over the past decades, prognosis of patients remains poor, with 5-year overall survival rates of 10% to 15% (27). Additionally, recent studies have indicated that immunosuppression is involved in oncogenicity, as well as tumor development and invasion in colorectal cancer (28, 29). The present study clarified the specific mechanism of the promotion of colorectal cancer tumorigenesis and metastasis by lncRNA MIR17HG, and we propose that it may serve as a promising immunotherapeutic target.

lncRNAs are functional transcripts that regulate gene expression through diverse mechanisms. Haurte has reviewed the roles of lncRNAs in the tumorigenesis and development of cancer and indicated that posttranscriptional regulation is one of the major molecular mechanisms by which lncRNAs function in a variety of human cancers (30). In the present study, we reported the posttranscriptional regulation of MIR17HG in the tumorigenesis of colorectal cancer in two ways. First, MIR17HG is the host gene for the miR-17-92 cluster, encoding a group of miRNAs (31); therefore, it induces gene silencing by binding to target sites within the 3′UTR of the targeted mRNA. Second, MIR17HG functions as a ceRNA and bases its activity on a sequence-specific interaction with miRNA, thus reducing their action on mRNA targets by titrating the amount of free miRNA (21).

The miR-17-92 cluster miRNAs encoded by MIR17HG are oncogenic miRNAs that have been studied in cancers (32, 33). The miR-17-92 miRNAs regulate genes involved in signaling molecules and the cell cycle (34, 35). In terms of colorectal cancer, it is reported that the miR-17-92 cluster is progressively accumulated during colorectal adenoma to adenocarcinoma progression and positively correlated to the aggressive phenotype of cancer (36). Ma and colleagues suggested that miR-17-5p promotes colorectal cancer development by targeting P130 (37). In addition, the expression level of miR-19a was significantly correlated with activated β-catenin in colorectal cancer and associated with the aggressive stage of tumor progression (38). In this study, we confirmed that the MIR17HG–miR-17-5p axis directly targeted BLNK, thus promoting the initiation and metastasis of colorectal cancer.

The tumor suppressor BLNK is a B-cell adaptor, and it plays an essential role in signal transduction by interacting with pre-B-cell and B-cell antigen receptors (39). BLNK-deficient mice show a high incidence of spontaneous pre-B-cell lymphoma due to enhanced proliferative capacity (40). Similarly, approximately 50% of human childhood pre-B acute lymphoblastic leukemia show the complete loss or a drastic reduction of BLNK expression (41). Here, we also confirmed the tumor suppressor role of BLNK in colorectal cancer.

lncRNAs can function as ceRNAs by competitively binding to miRNAs, thus positively regulating the target mRNAs (20, 21). We also determined that MIR17HG increased RELA expression without affecting miR-375 levels, indicating that MIR17HG behaves as a ceRNA. The RELA protein induces gene transcription by directly binding to the promoter region (42). In the ChIP assay, RELA directly bound to the promoter elements of MIR17HG, a positive feedback loop between MIR17HG and RELA was identified. RELA, which is constitutively activated in colorectal cancer, acts as a bridge between inflammation and cancer (43, 44). Liu and colleagues suggested that the miR-221/miR-222–RELA axis forms a positive feedback loop in colorectal cancer cells, promoting its malignant phenotypes (45). Despite the importance of RELA in colorectal cancer (46–48), it is not an ideally precise therapeutic target due to high cross-reactivity (49). Otherwise, our results suggested the targeting of MIR17HG as a potential therapeutic strategy for colorectal cancer. The lncRNA expression pattern is highly specific to tissue and cell type (50); therefore, drugs that target lncRNAs can be less toxic than conventional protein-targeting drugs (30).

Beyond these findings, we determined that MIR17HG directly bound to PD-L1 protein for accumulation in the colorectal cancer. T cell–based immunotherapy is a promising strategy for cancer treatment (51). PD-L1 is a key roadblock for T-cell activation, making it an ideal target for immunotherapy (51). Therefore, our study also highlighted the potential immunotherapeutic role of MIR17HG.

In summary, this study demonstrated that MIR17HG promotes tumorigenesis and metastasis in colorectal cancer via miR-17-5p to blunt BLNK. Meanwhile, MIR17HG and RELA are involved in positive feedback regulation through a ceRNA mechanism involving miR-375 in colorectal cancer. Furthermore, MIR17HG represents a potential immunotherapeutic target by binding to PD-L1. These findings may provide new

Published OnlineFirst August 13, 2019; DOI: 10.1158/0008-5472.CAN-18-3880

insights into the development of novel therapeutics for colorectal cancer.

Disclosure of Potential Conflicts of Interest

No potential conflicts of interest were disclosed.

Authors' Contributions

Conception and design: G. Familiari, M. Relucenti, H. Zhu, R. Chen
Development of methodology: H. Yang, H. Zhu, J. Wu
Acquisition of data (provided animals, acquired and managed patients, provided facilities, etc.): J. Xu, Q. Meng, X. Li, J. Xu, H. Sun, S. Wu, H. Zhu
Analysis and interpretation of data (e.g., statistical analysis, biostatistics, computational analysis): J. Xu, Q. Meng, N. Gao, H. Sun, S. Wu, G. Familiari, M. Relucenti, J. Wu
Writing, review, and/or revision of the manuscript: J. Xu, G. Familiari, M. Relucenti, H. Zhu, R. Chen
Study supervision: H. Zhu, R. Chen

Acknowledgments

This work was financially supported by the Fund of International Cooperation and Exchange of the National Natural Science Foundation of China (81861138017), the Ministry of Foreign Affairs and International Cooperation of Italy (PGR00962), the National Natural Science Foundation of China (91643109, 81730088, and 81703261), the Natural Science Foundation of Jiangsu Province (BK20171060), the Six Talent Peaks Project in Jiangsu Province (2016-WSN-002), the Fundamental Research Funds for the Central Universities, the Postgraduate Research and Practice Innovation Program of Jiangsu Province (KYCX17_0187 and KYCX18_0192).

The costs of publication of this article were defrayed in part by the payment of page charges. This article must therefore be hereby marked *advertisement* in accordance with 18 U.S.C. Section 1734 solely to indicate this fact.

Received December 10, 2018; revised April 10, 2019; accepted August 5, 2019; published first August 13, 2019.

References

1. Siegel RL, Miller KD, Jemal A. Cancer statistics, 2015. CA Cancer J Clin 2015;65:5–29.
2. Ullman TA, Itzkowitz SH. Intestinal inflammation and cancer. Gastroenterology 2011;140:1807–16.
3. Ruland J. Return to homeostasis: downregulation of NF-κB responses. Nat Immunol 2011;12:709–14.
4. Cooks T, Pateras IS, Tarcic O, Solomon H, Schetter AJ, Wilder S, et al. Mutant p53 prolongs NF-κB activation and promotes chronic inflammation and inflammation-associated colorectal cancer. Cancer Cell 2013;23:634–46.
5. Karin M, Greten FR. NF-κB: linking inflammation and immunity to cancer development and progression. Nat Rev Immunol 2005;5:749–59.
6. Ulitsky I, Bartel DP. lincRNAs: genomics, evolution, and mechanisms. Cell 2013;154:26–46.
7. Batista PJ, Chang HY. Long noncoding RNAs: cellular address codes in development and disease. Cell 2013;152:1298–307.
8. Schmitt AM, Chang HY. Long noncoding RNAs in cancer pathways. Cancer Cell 2016;29:452–63.
9. Kim T, Jeon YJ, Cui R, Lee JH, Peng Y, Kim SH, et al. Role of MYC-regulated long noncoding RNAs in cell cycle regulation and tumorigenesis. J Natl Cancer Inst 2015;107.
10. Ma Y, Yang Y, Wang F, Moyer MP, Wei Q, Zhang P, et al. Long non-coding RNA CCAL regulates colorectal cancer progression by activating Wnt/β-catenin signalling pathway via suppression of activator protein 2α. Gut 2016;65:1494–504.
11. Esposti DD, Hernandez-Vargas H, Voegele C, Fernandez-Jimenez N, Forey N, Bancel B, et al. Identification of novel long non-coding RNAs deregulated in hepatocellular carcinoma using RNA-sequencing. Oncotarget 2016;7:31862–77.
12. Yu X, Feng L, Liu D, Zhang L, Wu B, Jiang W, et al. Quantitative proteomics reveals the novel co-expression signatures in early brain development for prognosis of glioblastoma multiforme. Oncotarget 2016;7:14161–71.
13. Langfelder P, Horvath S. WGCNA: an R package for weighted correlation network analysis. BMC Bioinformatics 2008;9:559.
14. Duan H, Ge W, Zhang A, Xi Y, Chen Z, Luo D, et al. Transcriptome analyses reveal molecular mechanisms underlying functional recovery after spinal cord injury. PNAS 2015;112:13360–5.
15. Cioffi M, Trabulo SM, Sanchez-Ripoll Y, Miranda-Lorenzo I, Lonardo E, Dorado J, et al. The miR-17-92 cluster counteracts quiescence and chemoresistance in a distinct subpopulation of pancreatic cancer stem cells. Gut 2015;64:1936–48.
16. Jin HY, Oda H, Lai M, Skalsky RL, Bethel K, Shepherd J, et al. MicroRNA-17∼92 plays a causative role in lymphomagenesis by coordinating multiple oncogenic pathways. EMBO J 2013;32:2377–91.
17. Agnelli L, Forcato M, Ferrari F, Tuana G, Todoerti K, Walker BA, et al. The reconstruction of transcriptional networks reveals critical genes with implications for clinical outcome of multiple myeloma. Clin Cancer Res 2011;17:7402–12.
18. Fu C, Turck CW, Kurosaki T, Chan AC. BLNK: a central linker protein in B cell activation. Immunity 1998;9:93–103.
19. Oliveira-Costa JP, de Carvalho AF, da Silveira da GG, Amaya P, Wu Y, Park KJ, et al. Gene expression patterns through oral squamous cell carcinoma development: PD-L1 expression in primary tumor and circulating tumor cells. Oncotarget 2015;6:20902–20.
20. Cesana M, Cacchiarelli D, Legnini I, Santini T, Sthandier O, Chinappi M, et al. A long noncoding RNA controls muscle differentiation by functioning as a competing endogenous RNA. Cell 2011;147:947.
21. Salmena L, Poliseno L, Tay Y, Kats L, Pandolfi PP. A ceRNA hypothesis: the Rosetta Stone of a hidden RNA language? Cell 2011;146:353–8.
22. Tay Y, Rinn J, Pandolfi PP. The multilayered complexity of ceRNA crosstalk and competition. Nature 2014;505:344–52.
23. Wang F, Yuan JH, Wang SB, Yang F, Yuan SX, Ye C, et al. Oncofetal long noncoding RNA PVT1 promotes proliferation and stem cell-like property of hepatocellular carcinoma cells by stabilizing NOP2. Hepatology 2014;60:1278–90.
24. Couzin-Frankel J. Breakthrough of the year 2013. Cancer immunotherapy. Science 2013;342:1432–3.
25. Powles T, Eder JP, Fine GD, Braiteh FS, Loriot Y, Cruz C, et al. MPDL3280A (anti-PD-L1) treatment leads to clinical activity in metastatic bladder cancer. Nature 2014;515:558–62.
26. Bray F, Ferlay J, Soerjomataram I, Siegel RL, Torre LA, Jemal A. Global cancer statistics 2018: GLOBOCAN estimates of incidence and mortality worldwide for 36 cancers in 185 countries. CA Cancer J Clin 2018;68:394–424.
27. Chand M, Keller DS, Mirnezami R, Bullock M, Bhangu A, Moran B, et al. Novel biomarkers for patient stratification in colorectal cancer: A review of definitions, emerging concepts, and data. World J Gastrointest Oncol 2018;10:145–58.
28. Grady WM, Carethers JM. Genomic and epigenetic instability in colorectal cancer pathogenesis. Gastroenterology 2008;135:1079–99.
29. Yaghoubi N, Soltani A, Ghazvini K, Hassanian SM, Hashemy SI. PD-1/PD-L1 blockade as a novel treatment for colorectal cancer. Biomed Pharmacother 2019;110:312–8.
30. Huarte M. The emerging role of lncRNAs in cancer. Nat Med 2015;21:1253–61.
31. Kato M, Wang M, Chen Z, Bhatt K, Oh HJ, Lanting L, et al. An endoplasmic reticulum stress-regulated lncRNA hosting a microRNA megacluster induces early features of diabetic nephropathy. Nat Commun 2016;7:12864.
32. Olive V, Jiang I, He L. mir-17-92, a cluster of miRNAs in the midst of the cancer network. Int J Biochem Cell Biol 2010;42:1348–54.
33. Mirzamohammadi F, Kozlova A, Papaioannou G, Paltrinieri E, Ayturk UM, Kobayashi T. Distinct molecular pathways mediate Mycn and Myc-regulated miR-17-92 microRNA action in Feingold syndrome mouse models. Nat Commun 2018;9:1352.

Published OnlineFirst August 13, 2019; DOI: 10.1158/0008-5472.CAN-18-3880

34. Ventura A, Young AG, Winslow MM, Lintault L, Meissner A, Erkeland SJ, et al. Targeted deletion reveals essential and overlapping functions of the miR-17 through 92 family of miRNA clusters. Cell 2008;132:875–86.
35. Mestdagh P, Bostrom AK, Impens F, Fredlund E, Van Peer G, De Antonellis P, et al. The miR-17-92 microRNA cluster regulates multiple components of the TGF-β pathway in neuroblastoma. Mol Cell 2010;40:762–73.
36. Luo H, Zou J, Dong Z, Zeng Q, Wu D, Liu L. Up-regulated miR-17 promotes cell proliferation, tumour growth and cell cycle progression by targeting the RND3 tumour suppressor gene in colorectal carcinoma. Biochem J 2012;442:311–21.
37. Ma Y, Zhang P, Wang F, Zhang H, Yang Y, Shi C, et al. Elevated oncofoetal miR-17-5p expression regulates colorectal cancer progression by repressing its target gene P130. Nat Commun 2012;3:1291.
38. Li Y, Lauriola M, Kim D, Francesconi M, D'Uva G, Shibata D, et al. Adenomatous polyposis coli (APC) regulates miR17-92 cluster through β-catenin pathway in colorectal cancer. Oncogene 2016;35: 4558–68.
39. Grabbe A, Wienands J. Human SLP-65 isoforms contribute differently to activation and apoptosis of B lymphocytes. Blood 2006;108:3761–8.
40. Flemming A, Brummer T, Reth M, Jumaa H. The adaptor protein SLP-65 acts as a tumor suppressor that limits pre-B cell expansion. Nat Immunol 2003;4:38–43.
41. Jumaa H, Bossaller L, Portugal K, Storch B, Lotz M, Flemming A, et al. Deficiency of the adaptor SLP-65 in pre-B-cell acute lymphoblastic leukaemia. Nature 2003;423:452–6.
42. Hayden MS, Ghosh S. Shared principles in NF-κB signaling. Cell 2008;132: 344–62.
43. Ben-Neriah Y, Karin M. Inflammation meets cancer, with NF-κB as the matchmaker. Nat Immunol 2011;12:715–23.
44. Perkins ND. The diverse and complex roles of NF-κB subunits in cancer. Nat Rev Cancer 2012;12:121–32.
45. Liu S, Sun X, Wang M, Hou Y, Zhan Y, Jiang Y, et al. A microRNA 221- and 222-mediated feedback loop maintains constitutive activation of NFκB and STAT3 in colorectal cancer cells. Gastroenterology 2014;147:847–59. e11.
46. Lu YX, Ju HQ, Wang F, Chen LZ, Wu QN, Sheng H, et al. Inhibition of the NF-κB pathway by nafamostat mesilate suppresses colorectal cancer growth and metastasis. Cancer Lett 2016;380:87–97.
47. Qin M, Zhang J, Xu C, Peng P, Tan L, Liu S, et al. Knockdown of NIK and IKKβ-binding protein (NIBP) reduces colorectal cancer metastasis through down-regulation of the canonical NF-κB signaling pathway and suppression of MAPK signaling mediated through ERK and JNK. PLoS One 2017;12:e0170595.
48. Tian H, Qian J, Ai L, Li Y, Su W, Kong XM, et al. Upregulation of ASAP3 contributes to colorectal carcinogenesis and indicates poor survival outcome. Cancer Sci 2017;108:1544–55.
49. Yamamoto Y, Gaynor RB. Therapeutic potential of inhibition of the NF-κB pathway in the treatment of inflammation and cancer. J Clin Invest 2001; 107:135–42.
50. Iyer MK, Niknafs YS, Malik R, Singhal U, Sahu A, Hosono Y, et al. The landscape of long noncoding RNAs in the human transcriptome. Nat Genet 2015;47:199–208.
51. Wang RF, Wang HY. Immune targets and neoantigens for cancer immunotherapy and precision medicine. Cell Res 2017;27:11–37.

Cancer Research
The Journal of Cancer Research (1916–1930) | The American Journal of Cancer (1931–1940)

AACR American Association for Cancer Research

Long Noncoding RNA MIR17HG Promotes Colorectal Cancer Progression via miR-17-5p

Jie Xu, Qingtao Meng, Xiaobo Li, et al.

Cancer Res 2019;79:4882-4895. Published OnlineFirst August 13, 2019.